

# PSR J1740+1000: A Young Pulsar Well Out Of The Galactic Plane

M. A. McLaughlin<sup>1</sup>, Z. Arzoumanian<sup>2</sup>, J. M. Cordes<sup>1</sup>, D. C. Backer<sup>3</sup>,  
A. N. Lommen<sup>3</sup>, D. R. Lorimer<sup>4</sup>, & A. F. Zepka<sup>5</sup>

## ABSTRACT

We discuss PSR J1740+1000, one of five pulsars recently discovered in a search of 470 square degrees at 430 MHz during the upgrade of the 305-m Arecibo telescope. The period  $P = 154$  ms and period derivative  $\dot{P} = 2.1 \times 10^{-14}$  s s<sup>-1</sup> imply a spin-down age  $\tau_s = P/2\dot{P} = 114$  kyr that is smaller than 95% of all known pulsars. The youth and proximity of this pulsar make it a good candidate for detection at X-ray and gamma-ray energies. Its high Galactic latitude ( $b = 20.4^\circ$ ) suggests a very high velocity if the pulsar was born in the midplane of the Galaxy and if its kinematic age equals its spindown age. Interstellar scintillations, however, suggest a much lower velocity. We discuss possible explanations for this discrepancy, taking into account (a) possible birth sites away from the midplane; (b) contributions from the unmeasured radial velocity; (c) a kinematic age different from the spin-down age; and (d) biasing of the scintillation velocity by enhanced scattering from the North Polar Spur.

*Subject headings:* pulsars — pulsars:individual (J1740+1000) — ISM:individual (North Polar Spur)

## 1. Introduction

PSR J1740+1000, discovered in an Arecibo survey at 430 MHz, is a young pulsar at high Galactic latitude. It may be representative of a class of high-velocity pulsars which have

---

<sup>1</sup>Astronomy Department, Cornell University, Ithaca, NY 14853

<sup>2</sup>Laboratory for High-Energy Astrophysics, NASA-GSFC, Code 662, Greenbelt, MD 20771. NAS/NRC Research Associate

<sup>3</sup>Astronomy Department, University of California, Berkeley, CA 94720

<sup>4</sup>Arecibo Observatory, HC3 Box 53995, Puerto Rico 00612

<sup>5</sup>Currently at Numerical Technologies, 70 W. Plumeria Drive, San Jose, CA 95134-2134

thus far eluded detection. Determining the velocity and origin of this object is important as pulsar velocities represent fossil information about evolution of close binary systems and core collapse processes in supernovae. The largest velocities, in excess of  $1000 \text{ km s}^{-1}$ , provide the greatest constraints on such processes. Measuring pulsar velocities is also crucial for pulsar population statistics, determining the birth rate and birth places of pulsars and for planning future pulsar searches. Unfortunately, pulsar surveys have been strongly biased against the detection of high-velocity pulsars. While the average pulsar speed is about  $500 \text{ km s}^{-1}$ , the tail of the velocity distribution extends to at least  $1600 \text{ km s}^{-1}$ , with 10-20% of all pulsars having speeds greater than  $1000 \text{ km s}^{-1}$  (Lyne & Lorimer 1994; Cordes & Chernoff 1998; Arzoumanian et al. 2001). At these speeds, within a typical 10 Myr pulsar lifetime many high-velocity pulsars will have moved beyond the volume of detectability of previous surveys at low Galactic latitudes (Lorimer et al. 1997).

In §2 of this paper, we describe the search and follow-up observations. In §3, we present a timing model and discuss the pulsar’s single pulse and interstellar scintillation (ISS) properties. In §4, we explore ways to reconcile the kinematic and ISS velocities of the pulsar. In §5 and §6, we describe prospects for astrometry and high-energy detection, respectively. In §7, we present our main conclusions and plans for future study.

## 2. Observations

PSR J1740+1000 was discovered during the upgrade of the Arecibo Observatory, when several collaborations jointly surveyed the Arecibo sky (covering declinations roughly between  $-1^\circ$  and  $39^\circ$ ). As the telescope was not able to track sources, data were taken as the sky drifted through the beam at the sidereal rate. A point source drifts through the Arecibo 430-MHz  $10'$  beam in approximately 40 seconds. The feed was moved once a day to allow successive declination strips to be surveyed. The nominal sensitivity of this search, which employed 32 channels covering a bandwidth of 8 MHz, was approximately 0.5 mJy. We estimate that the techniques used for radio frequency interference excision and candidate evaluation raised our sensitivity to roughly 1 mJy. With a sampling interval of  $250 \mu\text{s}$ , we were sensitive to pulsars with periods  $\sim 1 \text{ ms}$  up to dispersion measures (DMs) of  $\sim 20 \text{ pc cm}^{-3}$  and to pulsars with periods  $\sim 30 \text{ ms}$  up to DMs of  $\sim 600 \text{ pc cm}^{-3}$ .

The Berkeley/Cornell collaboration covered 470 square degrees between 1994 October and 1995 February. We detected 5 new pulsars in the search. Three (J0030+0451, J0711+0931 and J1313+0931) were reported in Lommen et al. (2000), and two (J1740+1000 and J1849+2423) were reported in McLaughlin et al. (2000). With a search-derived period of 154 ms, a DM of  $\sim 20 \text{ pc cm}^{-3}$  and signal-to-noise ratio of  $\sim 20$ , J1740+1000 was one of

several pulsar candidates which were reobserved after the upgrade was completed. Confirming observations were done in May 1998 with the Arecibo Observatory Fourier Transform Machine (AOFTM), a Fourier transform-based spectrometer with 1024 10-kHz frequency channels and 102.4  $\mu$ s sampling<sup>6</sup>. The pulsar was timed from May 1999 onwards with the Penn State Pulsar Machine (PSPM), a filterbank with 128 60-kHz frequency channels and 80  $\mu$ s sampling. We have also observed this pulsar with the Wideband Arecibo Pulsar Processor (WAPP), a fast-dump digital correlator covering up to a 100 MHz bandwidth with a programmable number of lags and time resolution<sup>7</sup> (Dowd et al. 2000).

We mapped the field of this pulsar with the Very Large Array (VLA) in A array at 1.4 GHz using a 50-MHz bandwidth and 12-minute integration. At the time of these observations in July 1999, the pulsar’s position was known to approximately 3′ (i.e. one 1.4-GHz beam at Arecibo). We detected a continuum source in this observation with a flux density of  $2.26 \pm 0.17$  mJy at a position (J2000 = MJD 51385) of RA=17<sup>h</sup>40<sup>m</sup>25<sup>s</sup>.958  $\pm$  0.003, DEC=+10°00′05.91  $\pm$  0.05 (derived using the AIPS task JMFIT). Subsequent timing confirmed that this source was indeed the pulsar. The quoted 0.17 mJy error on the flux density does not account for fluctuations due to interstellar scintillation, which are significant. No other point sources were within 3′ of the position of PSR J1740+1000, but 2 sources, both listed in the NVSS catalog (Condon et al. 1998), were within 5′. No filamentary or bow-shock structures were visible in the radio maps.

### 3. Analysis and Results

#### 3.1. Pulsar Properties

We began regular timing observations of PSR J1740+1000 in May 1999 at an observing frequency of 430 MHz. After we established an initial timing model and more accurate position, timing observations were carried out predominantly at 1.4 GHz, where higher signal-to-noise profiles could be acquired. Pulse times-of-arrival (TOAs) were calculated by cross correlating dedispersed profiles with templates, using separate templates made from the addition of many individual pulses at both 430 MHz and 1.4 GHz. These TOAs were then analyzed using the TEMPO software package<sup>8</sup> (Taylor & Weisberg 1989). A timing solution for PSR J1740+1000, derived from 684 TOAs spanning almost two years, is presented in

---

<sup>6</sup><http://www.naic.edu/~aoftm>

<sup>7</sup><http://www.naic.edu/~wapp>

<sup>8</sup><http://pulsar.princeton.edu/tempo>

Table 1. With a spin-down age  $\tau_s$  of 114 kyr, this pulsar is younger than 95% of all pulsars listed in the Princeton Pulsar Catalog (Taylor et al. 1993). Given the  $23.85 \text{ pc cm}^{-3}$  DM of this pulsar, we use the Taylor & Cordes (1993) model for Galactic electron density (hereafter TC93) to derive a distance of  $1.4 \pm 0.4 \text{ kpc}$ .

Repeated observations have shown that this pulsar’s average flux density appears to be *higher* at 1.4 GHz than at 430 MHz, with a spectral index  $\alpha$  (where  $S_\nu \propto \nu^\alpha$  for an observing frequency  $\nu$ ) of  $0.9 \pm 0.1$ . We note that the spectral index estimate is highly contaminated by interstellar scintillation, especially refractive interstellar scintillation (RISS) which is uncorrelated between the two frequencies. We note in passing that flat spectral indices may be characteristic of young pulsars (Lorimer et al. 1995), though the Crab is a counter example to this.

As shown in Figure 1, the 1.4 GHz profile is composed predominantly of two conal pulse components, while at 430 MHz a core component is apparent. In Figure 2, we present a polarization profile based on WAPP observations carried out at 1475 MHz. The degree of linear polarization is 96%. Other pulsars with degrees of linear polarization greater than 80% include J0134–2937, B0136+57, J0631+1036, B0656+14, J0742–2822, B0740–28, B0833–45, B0906–49, B1259–63, J1359–6038, J1643–1224, B1737–30, B1913+167 and B1929+10 (McCulloch et al. 1978; Wu et al. 1993; Manchester & Johnston 1995; Xilouris & Kramer 1996; Zepka et al. 1996; Gould & Lyne 1998; Manchester et al. 1998; Weisberg et al. 1999). With some exceptions (most notably B1643–12 and B1913+167) these pulsars have similar ages and/or periods to PSR J1740+1000, supporting a possible correlation between the degree of linear polarization and period and/or age, as has been noted before (Manchester 1971; McCulloch et al. 1978; von Hoensbroech et al. 1998). From data taken over a 100-MHz bandwidth at 1.475 GHz, we derive a rotation measure of  $23.8 \pm 2.8 \text{ rad m}^{-2}$ . For a DM of  $23.85 \text{ pc cm}^{-3}$ , this translates to an average magnetic field along the line of sight of  $1.2 \pm 0.1 \mu\text{Gauss}$ .

Because the pulsar’s young age, estimated distance and high Galactic latitude suggest a high space velocity, a proper motion measurement is very desirable. However, the pulsar’s large timing residuals (see Figure 3), currently prohibit this. The scatter in these residuals is likely dominated by the considerable pulse-to-pulse jitter exhibited by this pulsar, as shown in Figure 4. At 1.4 GHz, both single-peaked and multiple-peaked pulse shapes are recognizable, with the single-peaked modes generally stronger. Sometimes a precursor, arriving  $\sim 10 \text{ ms}$  before the main pulse, is present. More infrequently, a stronger postcursor, arriving  $\sim 10 \text{ ms}$  after the main pulse, is apparent. An auto-correlation analysis shows that pulses are intrinsically modulated on timescales  $\sim 1 \text{ s}$  (i.e. 6-7 pulses), as shown in Figure 5. This timescale is similar at both 1.4 GHz and 430 MHz. The modulation index  $m$ , corrected for

additive off-pulse noise,

$$m = \frac{(\sigma_{\text{on}}^2 - \sigma_{\text{off}}^2)^{1/2}}{\langle I_{\text{on}} \rangle - \langle I_{\text{off}} \rangle}, \quad (1)$$

where  $\sigma_{\text{on}}$  and  $\sigma_{\text{off}}$  are the on- and off-pulse RMS and  $\langle I_{\text{on}} \rangle$  and  $\langle I_{\text{off}} \rangle$  are the average on- and off-pulse intensities, is calculated across the pulse and shown in Figure 6. The shape is similar to that calculated for other strongly modulated pulsars, with greater modulation on the outer edges of the pulse (Backer 1973; Bartel et al. 1980).

### 3.2. Velocities

We define the  $z$ -velocity of an object of “kinematic” age  $t$  born at height  $z_0$  above the Galactic plane as

$$V_z = \frac{z - z_0}{t}, \quad (2)$$

for a present-day height of  $z = D \sin b$ . For PSR J1740+1000, assuming  $z_0 = 0$ ,  $D = 1.4$  kpc and  $t = \tau_s$ , we find  $V_z = 4160 \text{ km s}^{-1}$ . Even for a  $z_0$  of 0.3 kpc, over twice the best-fit scale height of the pulsar progenitor population (Cordes & Chernoff 1998; Arzoumanian et al. 2001), a velocity of  $1500 \text{ km s}^{-1}$  is required for PSR J1740+1000 to have reached its present-day  $z$  of 0.48 kpc in its 114-kyr lifetime. Note that, even for velocities as large as  $4000 \text{ km s}^{-1}$ , contamination of  $\tau_s$  due to the Shklovskii effect (Shklovskii 1970) is insignificant, producing an apparent  $\dot{P}$  of roughly 1% of the true value. We later discuss the possibility that the kinematic age is much larger than the spin-down age. In Figure 7, we show  $V_z$  (for  $z_0$  of zero) for all pulsars in the Princeton Pulsar Catalog (Taylor et al. 1993) with latitude greater than 10 degrees. We chose this latitude cutoff to exclude pulsars within the progenitor scale height and pulsars seen through much of the Galactic disk, where uncertainties in TC93 are greater.

To relate an object’s  $z$ -velocity to its transverse velocity along of the line of sight, we adopt an  $(x, y, z)$  coordinate system such that  $x, y$  define the Galactic plane, with  $x$  towards longitude  $l = 90$  and  $y$  towards  $l = 180$ , and  $z$  is toward the North Galactic pole. We then let  $\hat{\mathbf{n}}$ ,  $\hat{\mathbf{l}}$  and  $\hat{\mathbf{m}}$  be unit vectors, with  $\hat{\mathbf{n}}$  along the line of sight to the pulsar,  $\hat{\mathbf{l}}$  and  $\hat{\mathbf{m}}$  transverse to the line of sight, and  $\hat{\mathbf{l}} \cdot \hat{\mathbf{z}} = 0$ , as in Eq. 28 of Cordes & Rickett (1998) (hereafter CR98). The pulsar’s true space velocity in the  $z$  direction is composed of radial and perpendicular components such that

$$V_z = V_{r,z} + V_{\perp,z} = V_r \sin b + V_{\perp,m} \cos b, \quad (3)$$

where  $V_{r,z}$  and  $V_{\perp,z}$  are the  $z$  components of the pulsar’s radial and transverse velocity, respectively, and  $V_{\perp,m}$  is the transverse velocity in the  $\hat{\mathbf{m}}$  direction. Assuming no radial velocity and  $z_0 = 0$ , we find  $V_{\perp,m} = 4430 \text{ km s}^{-1}$  for PSR J1740+1000. This is much higher

than the transverse velocity of  $1700 \text{ km s}^{-1}$  estimated for the fastest known pulsar, PSR B2224+65 (Cordes et al. 1993). However, it is entirely possible that the space velocity is much less than  $4430 \text{ km s}^{-1}$ , as we discuss below.

### 3.3. Interstellar Scintillation

One way to get an independent constraint on a pulsar’s velocity is through measurement of its interstellar scintillations (ISS). Because scattering by density inhomogeneities in the ionized interstellar medium causes multiple rays to interfere, it produces frequency structure in pulsar spectra (Scheuer 1968; Rickett 1990). These spectra change significantly on timescales of minutes to hours due to the high transverse velocities of most pulsars. When the spectrum is monitored over time, the resulting two-dimensional array or “dynamic spectrum” is often dominated by a random pattern of scintillation maxima with characteristic bandwidth and timescale (Rickett 1990). Intensity variations in time and frequency with scales of a few minutes and a few MHz are due to diffractive ISS (DISS), caused by small-scale irregularities in the interstellar plasma. Longer term intensity variations are caused by refractive ISS (RISS), due to variations in electron density on much larger scales than those responsible for DISS.

A two-dimensional correlation analysis can be used to calculate the scintillation bandwidth  $\Delta\nu_d$  and the scintillation timescale  $\Delta t_d$ , which quantify the interstellar scintillation properties of a pulsar. In Figure 8, we show an ACF of a dynamic spectrum for PSR J1740+1000. In Table 2 we list diffractive bandwidths and timescales measured from ACFs at various epochs. The average values of these parameters are  $\Delta t = 271 \text{ s}$  and  $\Delta\nu = 8.0 \text{ MHz}$ , with standard deviations of  $\sigma_{\Delta t} = 146 \text{ s}$  and  $\sigma_{\delta\nu} = 6.6 \text{ MHz}$ . The large variance in the scintillation parameters is likely due to a combination of measurement uncertainties (from small numbers of scintillation maxima in a given measurement) and modulation from RISS, which may be enhanced by refraction from the North Polar Spur (see below).

We may use these measurements to estimate the speed of the ISS diffraction pattern with respect to the observer. For a statistically uniform, Kolmogorov scattering medium, this speed can be calculated as (CR98, Eq. 13)

$$V_{\text{ISS},5/3,\text{u}} = A_{\text{ISS},5/3,\text{u}} \frac{\sqrt{D\Delta\nu_d}}{\nu\Delta t_d} \quad (4)$$

where  $A_{\text{ISS},5/3,\text{u}} = 2.53 \times 10^4 \text{ km s}^{-1}$  and  $D$ ,  $\Delta\nu_d$ ,  $\nu$  and  $\Delta t_d$  have units of kpc, MHz, GHz and s, respectively. We list  $V_{\text{ISS},5/3,\text{u}}$  for all epochs in Table 2 and, for a distance of 1.4 kpc, find an average value of  $216 \text{ km s}^{-1}$ , with a standard deviation of  $67 \text{ km s}^{-1}$ .

For a uniform, Kolmogorov medium,  $V_{\text{ISS},5/3,u}$  will be equal to the pulsar’s transverse speed. For other cases, making the reasonable assumption that the speeds of the observer and the medium are small compared to the pulsar’s, we may express the transverse speed of the pulsar as (CR98, Eq. 23)

$$V_{\perp} = W_C W_{\text{D,PM}} V_{\text{ISS},5/3,u}, \quad (5)$$

where the weighting factors  $W_C$  and  $W_{\text{D,PM}}$  relate the measured scintillation speed to the pulsar’s actual transverse speed. The contribution of  $W_C$ , which depends on both the wavenumber spectrum and the distribution of the medium (CR98, Eq. 18), is small (maximum range of 0.9-1.3). We therefore assume it is unity throughout the remaining analysis. The other factor,  $W_{\text{D,PM}}$ , is determined by the distribution of the scattering material along the line of sight to the pulsar. This is proportional to  $C_n^2$ , the coefficient of the electron-density wavenumber spectrum. An exact expression for  $W_{\text{D,PM}}$  for a square law phase structure function is given in CR98 (Eq. 25) as

$$\begin{aligned} W_{\text{D,PM}}(D) &= \left[ \frac{2 \int_0^D ds (s/D)(1-s/D) C_n^2(s)}{\int_0^D ds (1-s/D)^2 C_n^2(s)} \right]^{1/2} \\ &= \frac{SM_{\tau}^{1/2}}{[3SM - (SM_{\tau} + SM_{\theta})]^{1/2}} \end{aligned} \quad (6)$$

where  $s$ , the distance measured from the pulsar to the observer, varies from 0 to the pulsar distance  $D$  and

$$SM = \int_0^D ds C_n^2(s) \quad (7)$$

$$SM_{\tau} = 6 \int_0^D ds (s/D)(1-s/D) C_n^2(s) \quad (8)$$

$$SM_{\theta} = 3 \int_0^D ds (s/D)^2 C_n^2(s). \quad (9)$$

define the scattering measure, the scattering measure weighted for pulse broadening, and the scattering measure weighted for angular broadening, respectively.

If we use TC93 to calculate  $SM$ ,  $SM_{\tau}$  and  $SM_{\theta}$  and thus the weight factor  $W_{\text{D,PM}}$ , we find  $W_{\text{D,PM}} = 0.85$  and  $V_{\perp} = 184 \text{ km s}^{-1}$ , far smaller than the kinematic  $z$ -velocity calculated using  $z_0 = 0$  and  $t = \tau_s$ . In the following, we consider several ways to reconcile the various constraints on the pulsar’s velocity. Some reduce the value of the kinematic  $z$ -velocity while others increase the scintillation estimate of the transverse velocity. We note that, if the actual distance to the pulsar is much less than the distance estimated by TC93, the difference between the velocity estimated from ISS (proportional to  $\sqrt{D}$ ) and the kinematic velocity (proportional to  $D$ ) becomes smaller.

## 4. Interpretation of J1740+1000’s Kinematics

### 4.1. Large Radial Velocity

An unrealistically large radial velocity is required if we assume that it accounts solely for the difference between the  $V_z$  calculated assuming  $V_r = 0$  and the ISS speed, which reflects only the transverse components. Letting  $z$  be the pulsar’s height above the Galactic plane,  $z_{\text{TC}}$  the height above the plane given the TC93 model distance and ignoring any contribution to  $V_z$  from  $V_{\perp}$ , we have

$$\begin{aligned} V_r &\approx \left(\frac{D_{\text{TC}}}{\tau_s}\right) \left(\frac{\tau_s}{t}\right) \left(\frac{z - z_0}{z_{\text{TC}}}\right) \\ &\approx 1.2 \times 10^4 \text{ km s}^{-1} \left(\frac{\tau_s}{t}\right) \left(\frac{z - z_0}{z_{\text{TC}}}\right). \end{aligned} \quad (10)$$

Assuming that a value  $V_r \approx 10^3 \text{ km s}^{-1}$  is “reasonable” in comparison with the highest known velocities, it appears that either the pulsar is kinematically much older than the spindown age such that  $t \gg \tau_s$ , or the pulsar was born at a relatively high  $z_0$  such that  $|z - z_0| \ll z_{\text{TC}}$ . However, we later discuss other interpretations where the transverse velocity makes a sizeable contribution to  $V_z$  and  $V_r$  need not be so large.

### 4.2. Large Kinematic Age

Depending on the spindown law for the pulsar and on the evolutionary history of the neutron star’s progenitor, the spindown age  $\tau_s$  may or may not be a good estimate for the kinematic age  $t$ . First, the spindown age may only approximate the true age of the pulsar. Young pulsars show estimated braking indices  $n \equiv \Omega \ddot{\Omega} / \dot{\Omega}^2 < 3$ , where  $\Omega = 2\pi/P$ , implying ages greater than the spindown age  $\tau_s$ , which is calculated for  $n = 3$ . However, a pulsar born with spin period not significantly smaller than its present-day period could be much younger than  $\tau_s$ . In fact, a statistical comparison of kinematic  $z$ -velocities and proper motion derived velocities suggests that, on average, pulsars are about 50% *younger* than their spindown ages (Cordes & Chernoff 1998).

Recently, Gaensler & Frail (2000) argued that the pulsar PSR B1757–24 was significantly *older* than  $\tau_s$  by comparing the pulsar’s location to its birth place, estimated through identification of the geometric center of the associated supernova remnant. The upper bound on the proper motion of the synchrotron nebula around the pulsar suggests an older age. However, we believe that the errors associated with estimating ages based on remnant morphology are too large to allow any general statement about pulsar ages.



Secondly, even if the pulsar age is well approximated by  $\tau_s$ , the kinematic age could be significantly larger. For example, the progenitor of J1740+1000 may have been a member of a binary system whose primary exploded long before the observed pulsar was produced, imparting significant space velocities to its remnant star and to the progenitor of J1740+1000, either as an intact binary or as individual objects. A scenario of this type was proposed by Gott, Gunn & Ostriker (1970) to account for the current locations of the Crab pulsar (B0531+21) and the nearby, older and longer-period pulsar, B0525+21, with the binary producing both pulsars originating in the I Gem OB association.

### 4.3. Halo Progenitor

It is conceivable that PSR J1740+1000 may have been born well out of the Galactic plane from a halo-star progenitor, perhaps through a rare accretion induced collapse (AIC) or merger event (Bailyn & Grindlay 1990; Rasio & Shapiro 1995). If the neutron star formed through accretion induced collapse (AIC) of a halo white dwarf, the expected transverse speed would be  $\sim 250 \text{ km s}^{-1}$  (i.e. the characteristic speed of a halo star), in the absence of a supernova-induced kick. This is consistent with the scintillation estimate. Given one object in 114 kyr, a naïve estimate of the birth rate of such objects would be  $\sim 10^{-5} \text{ yr}^{-1}$ . This rate is about  $10^3$  times smaller than that of disk-born pulsars and about 3 – 10 times larger than the estimated birth rate of millisecond pulsars (Lorimer et al. 1995; Cordes & Chernoff 1997). Therefore, if AIC produces only large magnetic field objects, the birth rate implied by PSR J1740+1000 would be compatible with birth rates of other neutron star subpopulations. Because we have not accounted for any selection effects in detecting objects produced through AIC, this is of course a very rough estimate.

### 4.4. Interstellar Medium Structure and DISS

The local ISM has been sculpted by supernovae and stellar winds into shells and loops that could perturb both the pulsar’s distance estimate, which is based on the dispersion measure, and the scintillation parameters. If only the distance is in error, reconciliation of the DISS and kinematic velocities implies  $D \approx 4 \text{ pc}$  (for  $z_0 = 0$ ), which requires an unrealistically large HII column density within a few parsec of the Sun. For  $z_0 \neq 0$  the distance could be larger and a smaller fraction of DM would be needed from an HII region.

As shown in Figure 9, the line of sight to PSR J1740+1000 passes through the North Polar Spur (NPS) and the Gould Belt, an expanding disk of gas and young stars. The

North Polar Spur is the brightest part of the larger radio feature called Loop I, a  $116^\circ$  diameter circular feature on the sky centered at longitude  $330^\circ$  and latitude  $+18^\circ$ . The NPS rises from the Galactic plane at a longitude of  $30^\circ$  and covers latitudes of  $15 - 30^\circ$ , appearing as a bright, narrow ridge in radio and X-ray maps. Sofue (1977) postulates that the NPS is part of a shock front induced by an explosive event at the Galactic center. However, a local, supernova remnant origin for the NPS is usually assumed (Heiles et al. 1980; Salter 1983; Egger & Aschenbach 1995; Heiles 1998). Distance estimates given this assumption range from 50 to 200 pc (Berkhuijsen 1973; Bingham 1967), while the thickness of the NPS is estimated to be  $\sim 20$  pc (Berkhuijsen 1973). The distance of the Gould Belt in the direction of PSR J1740+1000 is 100 to 300 pc, also much less than the TC93 distance for PSR J1740+1000.

The discovery of PSR J1740+1000 may have implications for the long-standing question of how the NPS was formed. While it is generally accepted that such shells are produced through the release of energy into the interstellar medium, the age of the NPS is uncertain. Its slow rate of expansion indicates that it is fairly old, but the production of X-rays in the interior poses an apparent contradiction. If these X-rays are due to reheating processes, the NPS could be roughly  $2 \times 10^6$  years old and produced by one normal supernova explosion. However, if the X-ray emission is due to just a single event, the age of the NPS could be only  $2 \times 10^5$  years (Heiles et al. 1980), roughly the spin-down age of PSR J1740+1000.

Structure in the local ISM like that seen in the NPS and Gould Belt perturbs both DM and SM for the line of sight to the pulsar. Strong evidence for the diffracting and refracting power of the NPS comes from examining the distribution of Extreme Scattering Event (ESE) sources, extragalactic sources which show extreme variations in their radio light curves. ESEs are generally believed to be caused by strong diffraction and refraction due to enhanced electron density turbulence in the ISM. As shown in Figure 9, three of the ten known ESE sources (1749+096, 1821+107 & 1741-038) have lines of sight which pass near or through the North Polar Spur (Fey et al. 1996).

To proceed, we follow Chatterjee et al. (2001) by superposing a thin screen at distance  $D_s$  from the pulsar on a smoothly varying medium such as is modeled by TC93. This yields a DISS velocity correction factor

$$W_{\text{D,PM}}(D) = \frac{[6(D_s/D)(1 - D_s/D)\Delta\text{SM} + \text{SM}_\tau]^{1/2}}{[3(1 - D_s/D)^2\Delta\text{SM} + 3\text{SM} - (\text{SM}_\tau + \text{SM}_\theta)]^{1/2}}, \quad (11)$$

where  $\Delta\text{SM}$  is the additional scattering measure contributed by the screen. Given the standard definitions of SM and DM (i.e. Eq. 9 and  $\text{DM} = \int_0^D n_e(s)ds$ , where  $n_e$  is the electron density in the medium), we may relate  $\Delta\text{SM}$  and  $\Delta\text{DM}$ , the differential DM contributed by

the screen. For a screen of width  $\Delta s$ ,

$$\Delta\text{SM} = (1/3)(2\pi)^{-1/3} K_u F_s \frac{(\Delta\text{DM})^2}{\Delta s}, \quad (12)$$

where  $K_u = 10.2 \times 10^{-3} \text{m}^{-20/3} \text{cm}^6 \text{ kpc pc}^{-1}$  is a unit conversion factor, and the units of  $\Delta\text{SM}$ ,  $\Delta\text{DM}$ , and  $\Delta s$  are  $\text{kpc m}^{-20/3}$ ,  $\text{pc cm}^{-3}$  and  $\text{pc}$ , respectively. As defined in TC93,  $F_s$  is a dimensionless “fluctuation parameter” (i.e.  $C_n^2(s) \propto F_s n_e^2(s)$ ) which is found to range from 0.1 to 100 for the various Galactic components of the TC93 model. We note that while DM and SM are correlated, the excess electron density from a screen could cause a large fractional change in scattering measure but a much smaller fractional change in dispersion measure.

Given the SM,  $\text{SM}_\tau$ , and  $\text{SM}_\theta$  estimated by TC93 along the line of sight to the pulsar,  $W_{D,PM}$  will increase with increasing  $\Delta\text{SM}$ , asymptoting to a value of  $[2(D_s/D)/(1 - D_s/D)]^{1/2}$ . For the measured ISS velocity to be made consistent with  $z_0 = 0$  (assuming  $t = \tau_s$  and ignoring the radial velocity contribution to  $V_z$ ), a  $W_{D,PM}$  of 20.5 is needed. This requires an unreasonable  $D_s/D = 0.995$ , or, for a pulsar distance of 1.4 kpc, a screen that is only 7 pc away from the Earth. To calculate the minimum  $z_0$  for a range of realistic model parameters, we constrain  $\Delta\text{SM}$  such that the resultant  $\Delta\text{DM}$  is less than half of the pulsar’s DM. We note that  $\Delta\text{DM} = 11.9 \text{ pc cm}^{-3}$  corresponds to a screen electron density of  $0.6 \text{ cm}^{-3}$  for a screen thickness of 20 pc, roughly consistent with the constraint  $n_e \leq 0.4 \text{ cm}^{-3}$  derived by Heiles et al. (1980) from NPS rotation and emission measures. Assuming  $\Delta s$ ,  $D_s$ ,  $D$ , and  $F$  of 20 pc, 130 pc, 1.4 kpc, and 10, we calculate a minimum  $z_0$  of 0.34 kpc. Allowing screen distances as small as 50 pc, a pulsar distance as low as 0.6 kpc, a screen thickness as small as 10 pc, and a fluctuation parameter  $F_s$  as large as 1000, the lowest height at which the pulsar could have been born is 0.10 kpc, consistent with estimated distances to the NPS. Note that these minimum values of  $z_0$  depend on the assumption that there is no radial contribution to the transverse velocity and that the kinematic age is equal to the spin-down age.

#### 4.5. Refractive Modulation of DISS

Another effect of a strong phase screen is that it can refract the radiation into a cone of received directions that is not centered on the direct ray path between pulsar and observer. The result is to decrease the DISS bandwidth while leaving the DISS time scale unchanged (Cordes, Pidwerbetsky & Lovelace 1986). It is therefore possible that strong RISS is contaminating our measured  $\Delta\nu_d$ , causing an underestimate of  $V_{ISS,5/3,u}$ . For the  $V_{ISS,5/3,u}$  estimate to agree with the  $V_\perp$  estimated assuming  $V_r = 0$ ,  $z_0 = 0$  and  $t = \tau_s$ , the actual bandwidth, unperturbed by RISS, would have to be an impossibly high 3360 MHz. However, while RISS

may not be solely responsible for the discrepancy between the pulsar’s age and height above the plane and the measured scintillation parameters, it could be biasing our results. The distribution of ESE sources provides strong evidence for the refracting properties of the NPS.

## 5. Prospects for Astrometry

The most robust way to determine the velocity and possible origin of PSR J1740+1000 is through measurement of a proper motion and parallax. An estimated distance of 1.4 kpc corresponds to a parallax of 0.71 mas. A transverse speed of  $10^3 \text{ km s}^{-1}$  for a pulsar at that distance corresponds to a proper motion  $\sim 150 \text{ mas yr}^{-1}$ .

Because the timing residuals of the pulsar are large, the prospects for measuring the proper motion through VLBI are much better than through timing. Given the current RMS timing residuals, we estimate that we could expect to measure a  $150 \text{ mas yr}^{-1}$  proper motion to about 10 sigma with two more years of timing data. However, if there is significant timing noise, as is expected for a young pulsar, a proper motion may be unmeasurable. A parallax measurement through timing is not feasible.

The current Very Large Baseline Array (VLBA) has sufficient angular resolution to easily measure the anticipated proper motion. However, the  $\sim 2 \text{ mJy}$  1.4-GHz average flux density of this pulsar necessitates more collecting area than is available with the VLBA alone. With the addition of Arecibo and the GBT to the array, a proper motion should be measurable within several months. Moreover, we have seen episodes of scintillation enhancement of the pulsar’s flux density for sustained times ( $\sim 1 \text{ hr}$ ) by a factor of ten, which will boost the astrometric sensitivity of VLBI measurements. As in the case of PSR B0919+06 (Chatterjee et al. 2001), the situation may also be aided by the presence of two nearby calibrators with separations and flux densities of 4 and 5 arcminutes and 2.7 and 2.6 mJy, respectively (Condon et al. 1998). The in-beam calibrators may also allow measurement of the pulsar’s parallax, especially if the pulsar is associated with the nearby NPS or Gould Belt.

## 6. High-Energy Emission

Because of its youth and proximity, PSR J1740+1000 is an excellent candidate for detection at high energies. Assuming that X-ray flux is proportional to  $\dot{E}/D^2$  (Becker & Trümper 1997), where  $\dot{E}$  is the spin-down energy loss rate, PSR J1740+1000 has the 10th highest predicted X-ray flux out of 547 pulsars in the Princeton Pulsar Catalog (Taylor et al. 1993). Upcoming

observations with *Chandra* may reveal the existence of thermal or magnetospheric radiation from the star. Nebular emission from a compact synchrotron nebula or a pulsar wind nebula bow-shock, especially likely if the velocity of the pulsar is high, should be detectable.

This pulsar should also be a strong gamma-ray source. Given the model of McLaughlin & Cordes (2000), PSR J1740+1000 ranks 20th out of 547 pulsars for OSSE ( $50 \leq E \leq 200$  keV) flux and 10th out of 547 pulsars for EGRET ( $E > 100$  MeV) flux. Because this pulsar was not detected as an EGRET point source (Hartman et al. 1999), we can place an upper limit on its gamma-ray flux of  $8.7 \times 10^{32}$  ergs  $s^{-1}$   $kpc^{-2}$ , just above the flux of  $8.1 \times 10^{32}$  ergs  $s^{-1}$   $kpc^{-2}$  predicted by the McLaughlin & Cordes model. Unfortunately, even in the closest EGRET viewing period, PSR J1740+1000 is 20 degrees off-axis. Still, we did search this and other viewing periods for periodicities over a range of periods and period derivatives close to that predicted by our current timing model. To do this, we first created a barycentered time series of photon arrival times given the known position of the pulsar. Photons are then individually weighted by the EGRET point spread function and folded for each trial ephemeris. The point spread function weighting procedure produces a dramatic improvement in signal-to-noise. For each profile, we use the Bayesian procedure presented in McLaughlin et al. (1999) to calculate the probability of a pulse of unknown width and phase. Using this method, we detect the known EGRET pulsars with high signal-to-noise. While, not surprisingly, we find no convincing pulsed signatures for PSR J1740+1000, this pulsar should be easily detectable, modulo any beaming effects, with the Gamma-Ray Large Area Space Telescope (GLAST), with a projected sensitivity of  $3 \times 10^{31}$  ergs  $s^{-1}$   $kpc^{-2}$ . Gamma-ray observations of this pulsar will be aided greatly by its high latitude, where the Galactic gamma-ray background is much smaller than in the Galactic plane.

## 7. Conclusions

PSR J1740+1000 is a young pulsar whose study will yield important information about pulsar velocities and the local interstellar medium. As a young object at a high Galactic latitude, its existence may signify a complex progenitor history, either from a Galactic disk population or from a halo population. Alternatively, it may simply have an especially high velocity.

Using simple models, it is difficult to reconcile the measured scintillation properties of this pulsar with its age and height above the Galactic plane. While it is of course possible that this pulsar was indeed born out of the Galactic plane, there are several ways in which the measured ISS parameters could be reconciled with a birth in the midplane of the Galaxy. Clearly the best way to resolve this issue is through measurement of the proper motion and

parallax. With the upcoming addition of Arecibo and the GBT to the VLBA, a proper motion will be measurable within a few months. Measurement of the parallax will rely heavily on the quality of nearby calibrator sources and exploitation of strong scintillation maxima that boost the apparent flux density of the pulsar by a factor of ten or more. We are also planning high-energy observations with *Chandra* and GLAST, as, due to its youth and proximity, the pulsar should be a strong high-energy source.

We thank Shami Chatterjee for useful discussions. This work was partially supported by NSF grant AST-9819931. The work was also supported by the National Astronomy and Ionosphere Center, which is operated by Cornell University under cooperative agreement with the National Science Foundation (NSF). Part of this work was performed while ZA held a National Research Council Research Associateship Award at NASA-GSFC. We acknowledge the use of NASA's SkyView facility (<http://skyview.gsfc.nasa.gov>) located at NASA Goddard Space Flight Center.

## REFERENCES

- Arzoumanian, Z., Chernoff, D. F., & Cordes, J. M., 2001, ApJ, submitted, astro-ph/0106159
- Backer, D. C. 1973, ApJ, 182, 245
- Bailyn, C. D. & Grindlay, J. E. 1990, ApJ, 353, 159
- Bartel, N., Sieber, W., & Wolszczan, A. 1980, A&A, 90, 58
- Becker, W. & Trümper, J. 1997, A&A, 326, 682
- Berkhuijsen, E. M. 1973, A&A, 24, 143
- Bingham, R. G. 1967, MNRAS, 137, 157
- Chatterjee, S., Cordes, J. M. Lazio, T. J. W. Goss, W. M. Fomalont, E. B. & Benson, J. M. 2001, ApJ, 549
- Condon, et al. 1998, AJ, 115, 1693
- Cordes, J. M. & Helfand, D. J. 1980, ApJ, 239, 640
- Cordes, J. M., Pidwerbetsky, A. & Lovelace, R. V. E. L. 1986, ApJ, 310, 737
- Cordes, J. M., Romani, R. W., & Lundgren, S. C. 1993, Nature, 362, 133

- Cordes, J. M., & Chernoff, D. F., 1997, *ApJ*, 482, 971
- Cordes, J. M. & Chernoff, D. F. 1998, *ApJ*, 505, 315
- Cordes, J. M., & Rickett, B. J. 1998, *ApJ*, 507, 846
- Dowd, A., Sisk, W., & Hagen, J. 2000, *ASP Conf. Ser. 202: IAU Colloq. 177: Pulsar Astronomy - 2000 and Beyond*, 275
- Egger, R. J. & Aschenbach, B. 1995, *A&A*, 294, L25
- Fey, A. L., Clegg, A. W., & Fiedler, R. L. 1996, *ApJ*, 468, 543
- Gaensler, B. M. & Frail, D. A. 2000, *Nature*, 406, 158
- Gould, D. M. & Lyne, A. G. 1998, *MNRAS*, 301, 235
- Hartman, R. C. et al. 1999, *ApJS*, 123, 79
- Haslam, C. G. T., Stoffel, H., Salter, C. J., & Wilson, W. E. 1982, *A&AS*, 47, 1
- Heiles, C., Chu, Y. -, Troland, T. H., Reynolds, R. J., & Yegingil, I. 1980, *ApJ*, 242, 533
- Heiles, C. 1998, *Berlin Springer Verlag Lecture Notes in Physics*, v.506, 506, 229
- Gott, J. R. I., Gunn, J. E., & Ostriker, J. P. 1970, *ApJ*, 160, L91
- Lommen, A. N., Zepka, A., Backer, D. C., McLaughlin, M., Cordes, J. M., Arzoumanian, Z., & Xilouris, K. 2000, *ApJ*, 545, 1007
- Lorimer, D. R., Yates, J. A., Lyne, A. G., & Gould, D. M. 1995, *MNRAS*, 273, 411
- Lorimer, D. R., Bailes, M., & Harrison, P. A. 1997, *MNRAS*, 289, 592
- Lyne, A. G. & Lorimer, D. R. 1994, *Nature*, 369, 127
- Manchester, R. N. 1971, *ApJS*, 23, 283
- Manchester, R. N. & Johnston, S. 1995, *ApJ*, 441, L65
- Manchester, R. N., Han, J. L., & Qiao, G. J. 1998, *MNRAS*, 295, 280
- McCulloch, P. M., Hamilton, P. A., Manchester, R. N., & Ables, J. G. 1978, *MNRAS*, 183, 645
- McLaughlin, M. A., Cordes, J. M., Hankins, T. H., & Moffett, D. A. 1999, *ApJ*, 512, 929

- McLaughlin, M. A., Arzoumanian, Z., & Cordes, J. M., 2000, In ASP Conf. Ser. 202, Pulsar Astronomy - 2000 and Beyond, ed. M. Kramer, N. Wex, & R. Weilebinksi, (San Fransisco: ASP) pg. 41
- McLaughlin, M. A. & Cordes, J. M. 2000, ApJ, 538, 818
- Rasio, F. A. & Shapiro, S. L. 1995, ApJ, 438, 887
- Rickett, B. J., 1990, ARA&A, 28, 561
- Salter, C. J. 1983, Bulletin of the Astronomical Society of India, 11, 1
- Scheuer, P. A. G., 1968, Nature, 218, 920
- Shklovskii, I. S. 1970, Soviet Astronomy, 13, 562
- Sofue, Y. 1977, A&A, 60, 327
- Taylor, J. H. & Weisberg, J. M. 1989, ApJ, 345, 132
- Taylor, J. H., Manchester, R. N., & Lyne, A. G. 1993, ApJS, 88, 529
- Taylor, J. H. & Cordes, J. M. 1993, ApJ, 411, 674
- von Hoensbroech, A., Kijak, J., & Krawczyk, A. 1998, A&A, 334, 571
- Weisberg, J. M. et al. 1999, ApJS, 121, 171
- Wu, X., Manchester, R. N., Lyne, A. G., & Qiao, G. 1993, MNRAS, 261, 630
- Xilouris, K. M. & Kramer, M. 1996, ASP Conf. Ser. 105: IAU Colloq. 160: Pulsars: Problems and Progress, 245
- Zepka, A., Cordes, J. M., Wasserman, I., & Lundgren, S. C. 1996, ApJ, 456, 305



Table 2. DISS Parameters Measured at 1.4 GHz for  
PSR J1740+1000

MJD	$\Delta\nu_d$ (MHz)	$\Delta t_d$ (s)	$V_{\text{ISS},5/3,\text{u}}$ (km s <sup>-1</sup> )
51314	1.8	85	329
51674	2.4	226	147
51722	2.0	193	157
51851	16.0	372	226
51968	5.4	211	231
51986	16.4	537	157
52022	11.7	273	262

Table 1. Observed and Derived Parameters for PSR J1740+1000

Parameter	Value
Right Ascension (J2000)	17 <sup>h</sup> 40 <sup>m</sup> 25 <sup>s</sup> .950(5)
Declination (J2000)	+10°00′06″.3(2)
Galactic longitude	34.01067(7)°
Galactic latitude	+20.26828(5)°
Barycentric Period (s)	0.154087174313(2)
Period derivative ( $10^{-15}$ s s <sup>-1</sup> )	21.4651(2)
Epoch (MJD)	51662
Dispersion Measure (pc cm <sup>-3</sup> )	23.85(5)
Rotation Measure (rad m <sup>-2</sup> )	23.8(2.8)
Timing data span (MJD)	51310–52014
Number of TOAs	684
Post-fit RMS timing residual ( $\mu$ s)	952
Flux density at 0.4 GHz (mJy)	3.1(2)
Flux density at 1.4 GHz (mJy)	9.2(4)
Mean spectral index	0.9(1)
Distance* (kpc)	1.4
Dipole magnetic field strength <sup>†</sup> $B$ ( $10^{12}$ G)	1.8
Characteristic age <sup>†</sup> $\tau_s$ (kyr)	114

Note. — Figures in parentheses represent  $1\sigma$  uncertainties in least-significant digits quoted.

\*Calculated using the TC93 model

<sup>†</sup>Calculated using the standard magnetic dipole formulae viz:  $B = 3.2 \times 10^{19} \sqrt{P\dot{P}}$  Gauss;  $\tau = P/2\dot{P}$  (Manchester & Taylor 1977)

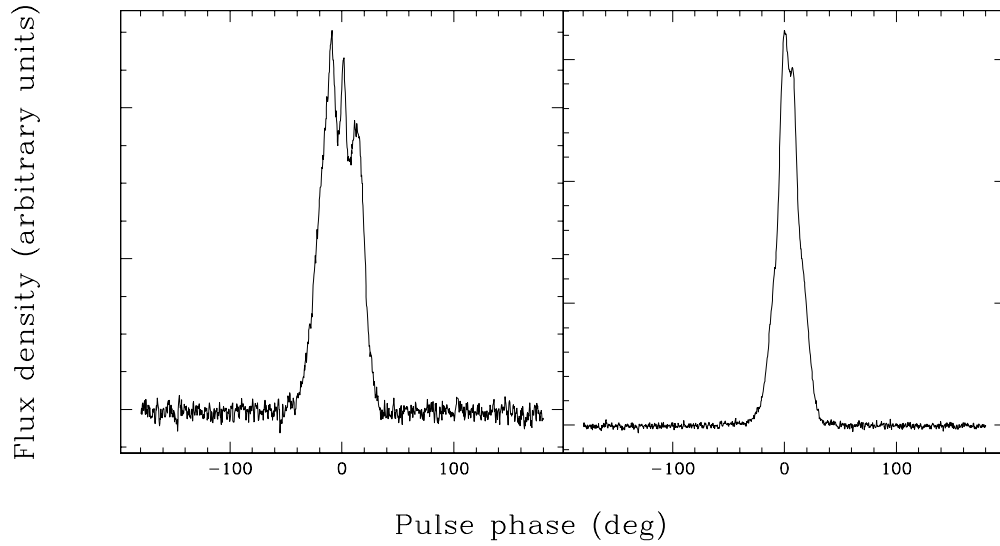


Fig. 1.— Folded pulse profiles for PSR J1740+1000 at 430 MHz (left) and 1.4 GHz (right). These profiles were formed by co-adding 17000 s and 11000 s of PSPM data at 430 MHz and 1.4 GHz, respectively. For all observations, data were taken across an 8-MHz bandwidth and dedispersed offline using a DM of  $23.85 \text{ pc cm}^{-3}$ .

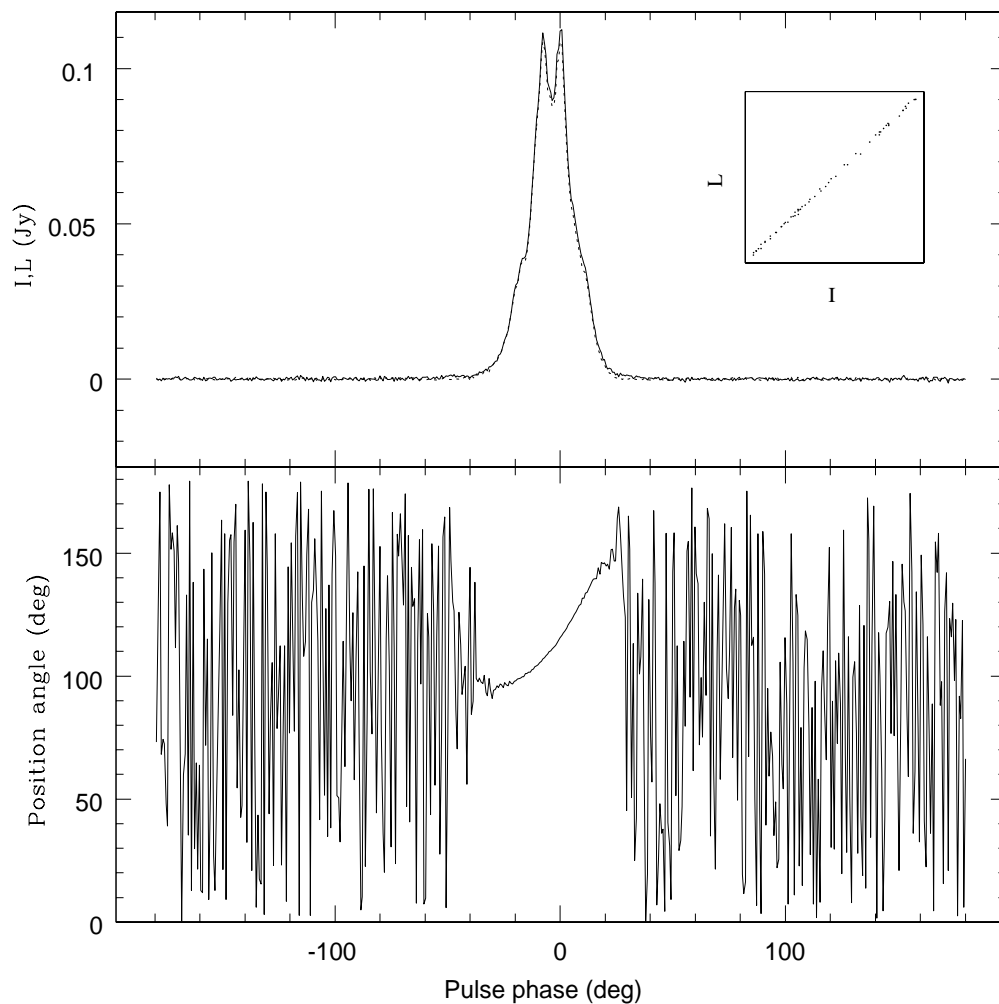


Fig. 2.— Polarization profile of PSR J1740+1000 at 1475 MHz. The upper panel shows the total intensity  $I$  (solid line) and linearly polarized intensity  $L$  (dashed line). These lines are nearly indistinguishable due to the high degree of linear polarization. Because this profile was formed from only 4 minutes of data, the pulse shape has not yet converged to that shown in Figure 1. The inset plot shows  $L$  vs.  $I$  across the pulse. The lower panel shows the polarization position angle. We do not show the circularly polarized power because it is influenced by the unknown cross coupling of the feed system.

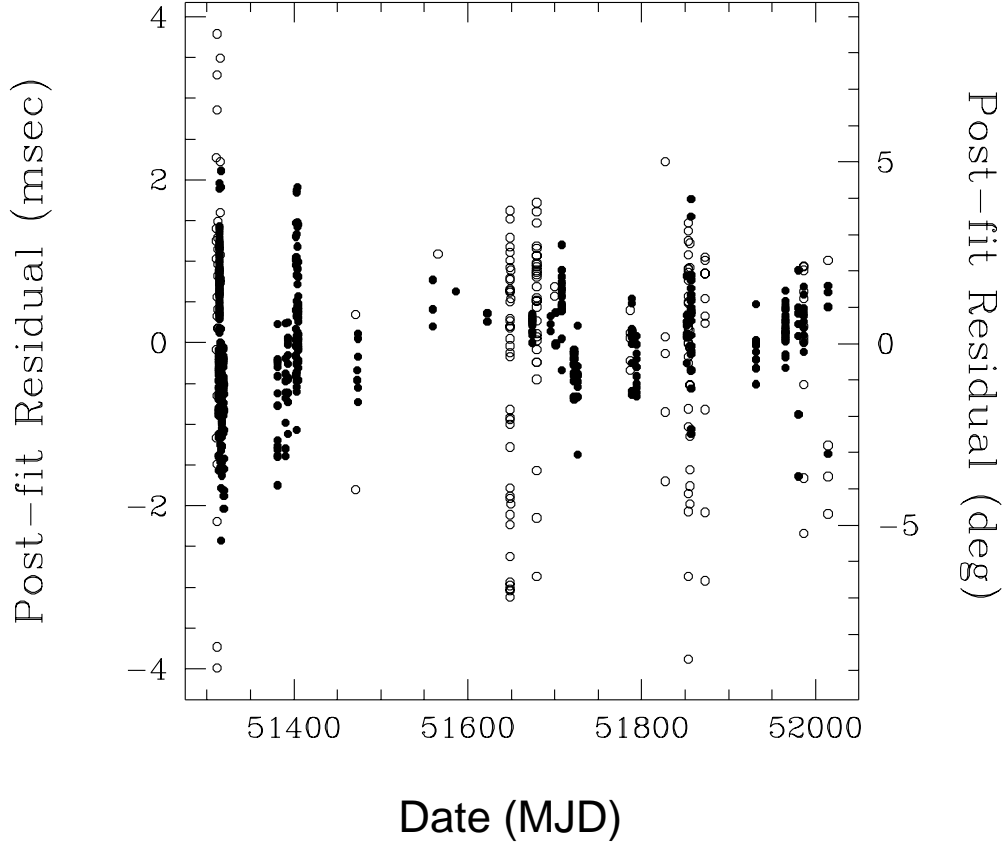


Fig. 3.— Timing residuals for 684 TOAs spanning MJDs 51310 to 52014 for the timing model in Table 1, which includes a fit for  $P$ ,  $\dot{P}$ , DM, RA and DEC. Fitting for proper motion or a frequency second derivation improves the fit somewhat, but since we are unsure of the origin of the long-term trend, we do not include it here. Open and closed circles denote measurements at 430 MHz and 1.4 GHz, respectively. TOA uncertainties range from 0.5 to 5 ms at 430 MHz and from 0.3 to 3 ms at 1.4 GHz, varying by an order of magnitude or more due to scintillation and profile shape variations. Note that, despite the variation in TOA uncertainty, all TOAs were given equal weight in the least-squares fit to minimize biasing from profile shape variations between individual scans.

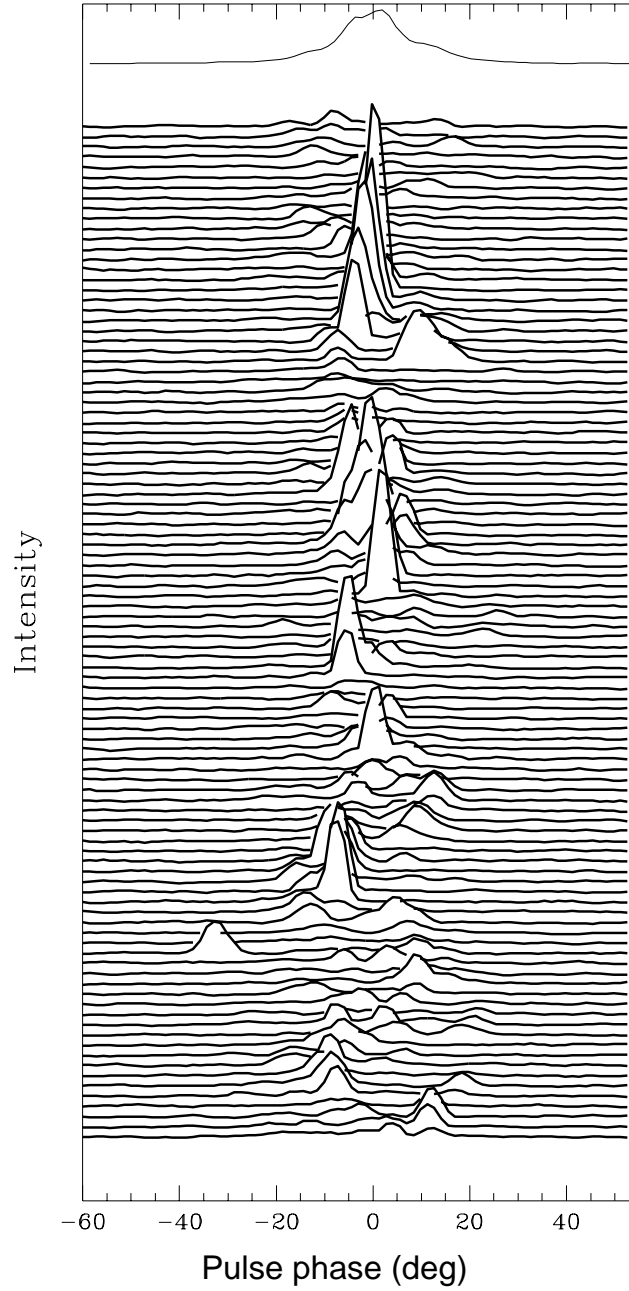


Fig. 4.— A sequence of 100 single pulses (i.e.  $\sim 15$  seconds of data) from PSR J1740+1000. These data were taken using the WAPP at 1.475 GHz across a 100-MHz bandwidth. The time resolution is 0.8 ms.

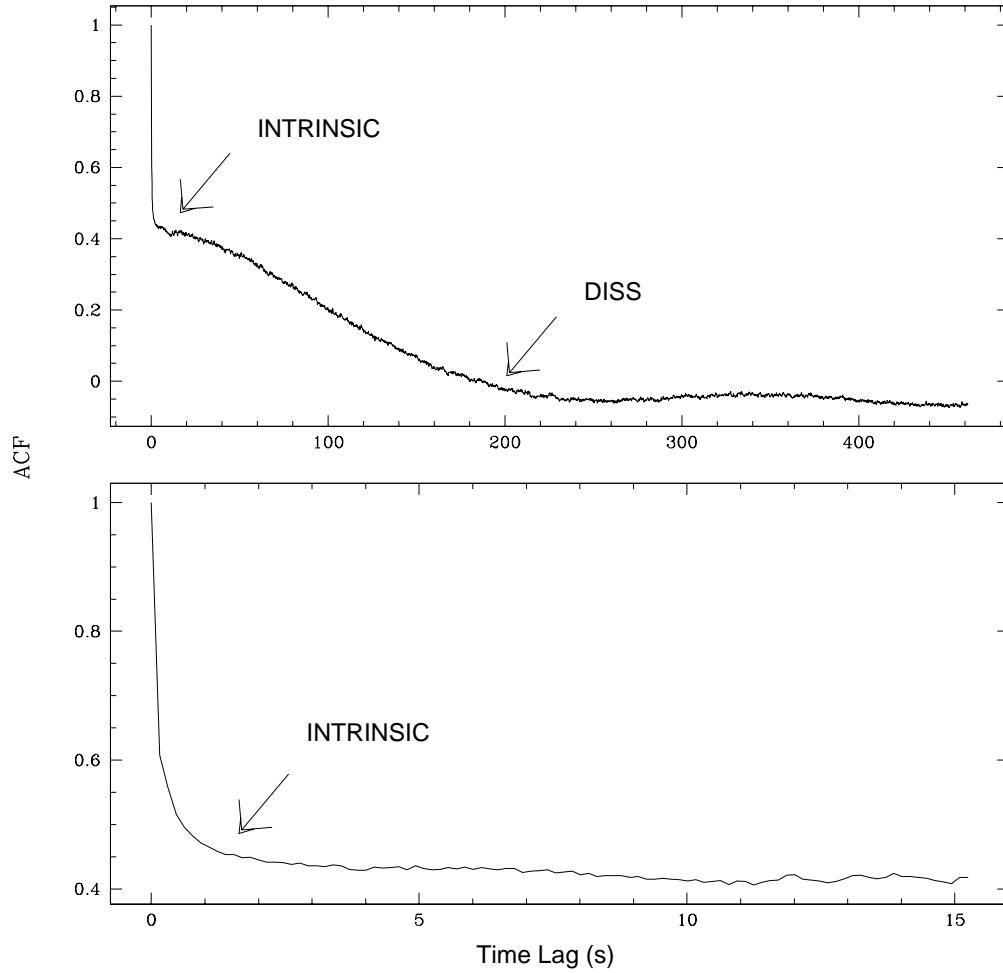


Fig. 5.— Auto-correlation function (ACF) for a dedispersed time series of period-averaged intensities for PSR J1740+1000. These data were taken with the AOFTM at 1.4 GHz across a 10-MHz bandwidth. The lower plot shows only the first 16 seconds. The variation with timescale  $\sim 200$  s is caused by diffractive interstellar scintillation (DISS), while the  $\sim 1$  s variation is due to intrinsic pulse-to-pulse fluctuations.

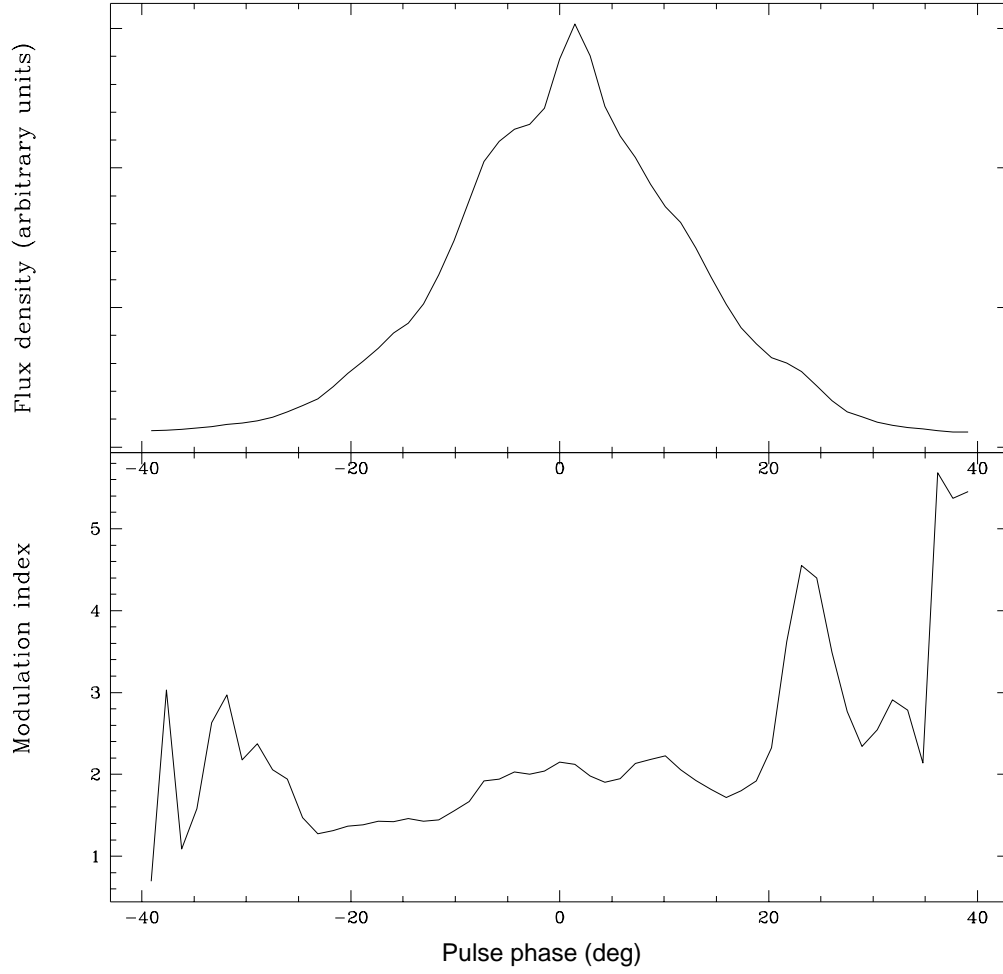


Fig. 6.— The inner 20% of the 1.475 GHz pulse profile, along with the corresponding modulation index, is shown for the full 1200-second observation from which the sequence in Figure 4 was taken.



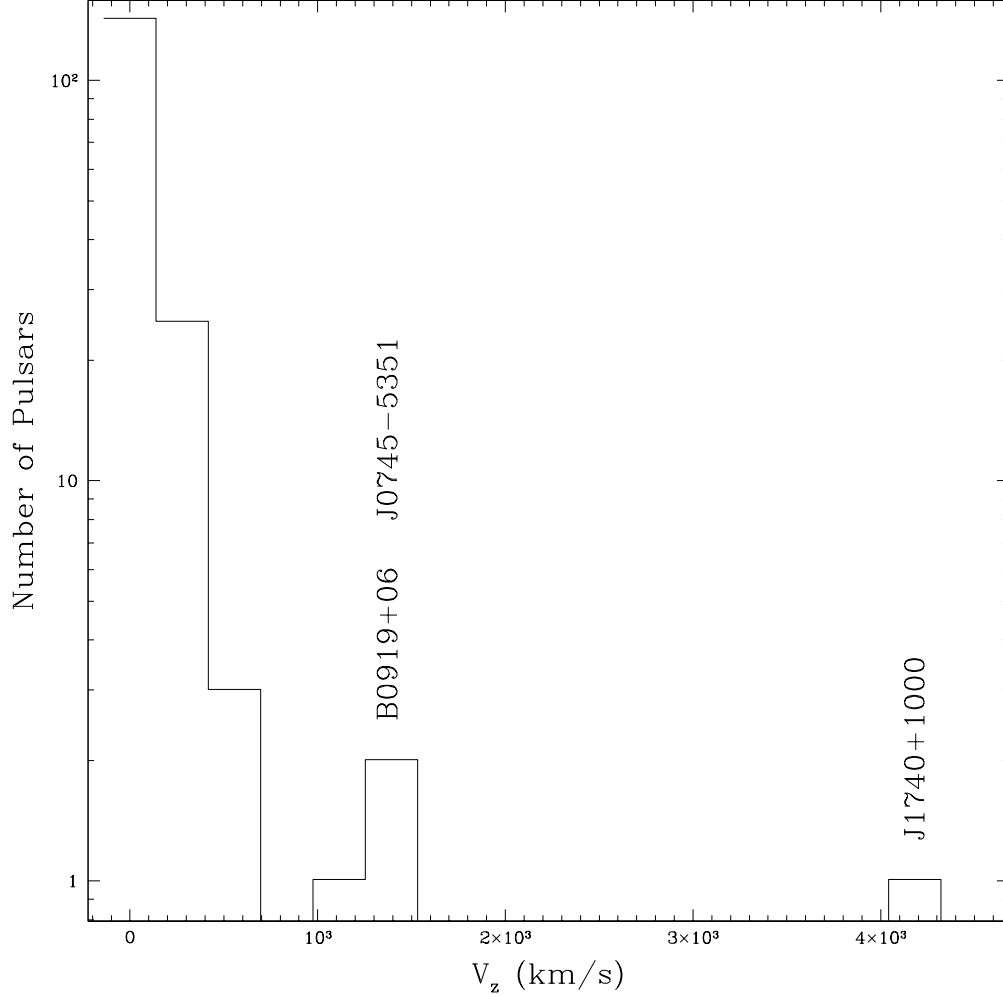


Fig. 7.—  $V_z$  is plotted for all pulsars in the Princeton Pulsar Catalog (Taylor et al. 1993) with Galactic latitudes  $|b| > 10^\circ$ . Note the logarithmic scaling of the y-axis. The value for PSR J1740+1000 is anomalously high. Pulsar distances were calculated using TC93, except in cases of a more accurate parallax measurement. We note that  $V_z$  can be quite different from measured transverse velocities. For instance, PSR B0919+06 has a  $V_z$  of  $1400 \text{ km s}^{-1}$ , but an astrometrically-determined transverse velocity of  $505 \pm 80 \text{ km s}^{-1}$  (Chatterjee et al. 2001). We also note that imposing a latitude cutoff omits pulsars such as PSR B0531+21 and PSR B1509-58, which have  $V_z$ s of  $1.6 \times 10^5$  and  $5.6 \times 10^4 \text{ km s}^{-1}$ , respectively, but, with known supernova remnant associations, were certainly born at  $|z_0| > 0$ .

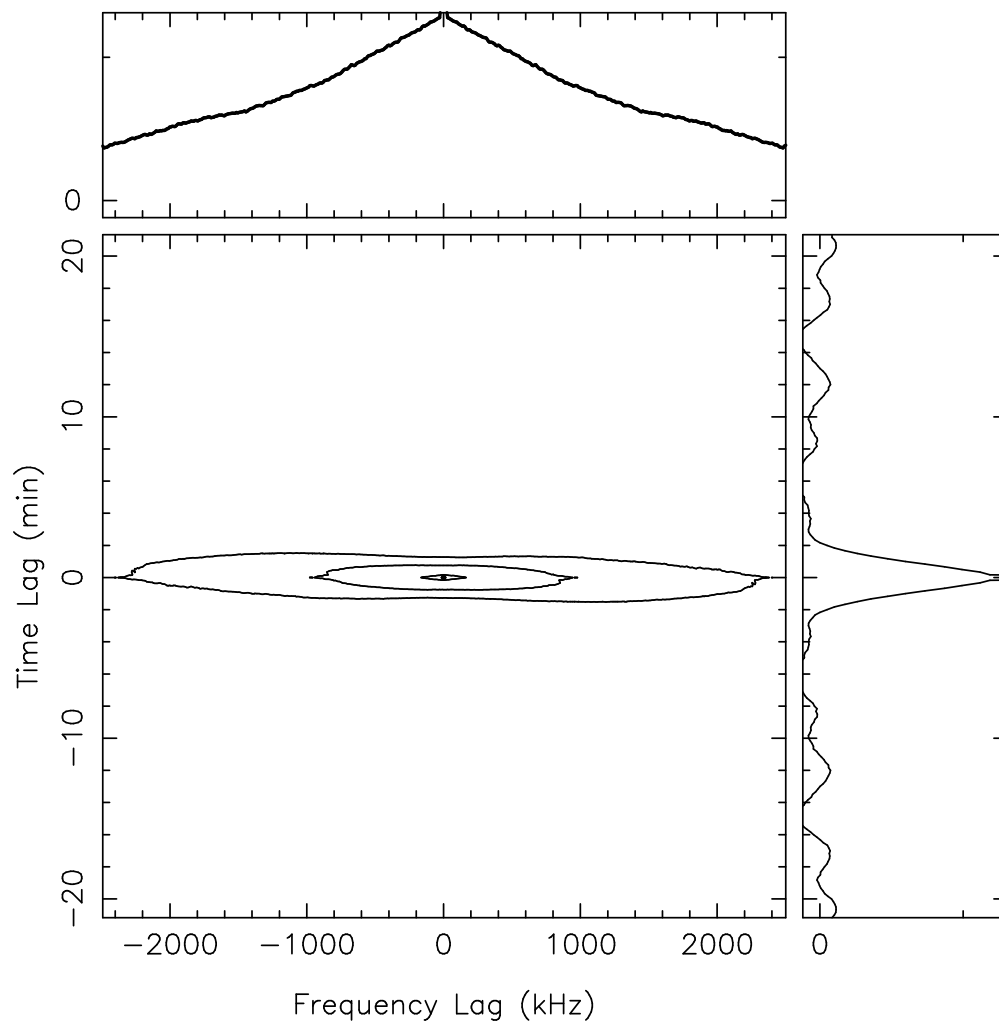


Fig. 8.— A two-dimensional ACF for a dynamic spectrum for PSR J1740+1000 taken at a center frequency of 1410 MHz in May 1999. We also plot one dimensional slices along the two axes, used to calculate  $\Delta\nu_d$  (as the half-width at half-max of the cut at zero time lag) and  $\Delta t_d$  (as the half width at  $e^{-1}$  of the cut at zero frequency lag). For this epoch, we calculate  $\Delta\nu_d = 85$  s and  $\Delta t_d = 1.8$  MHz.

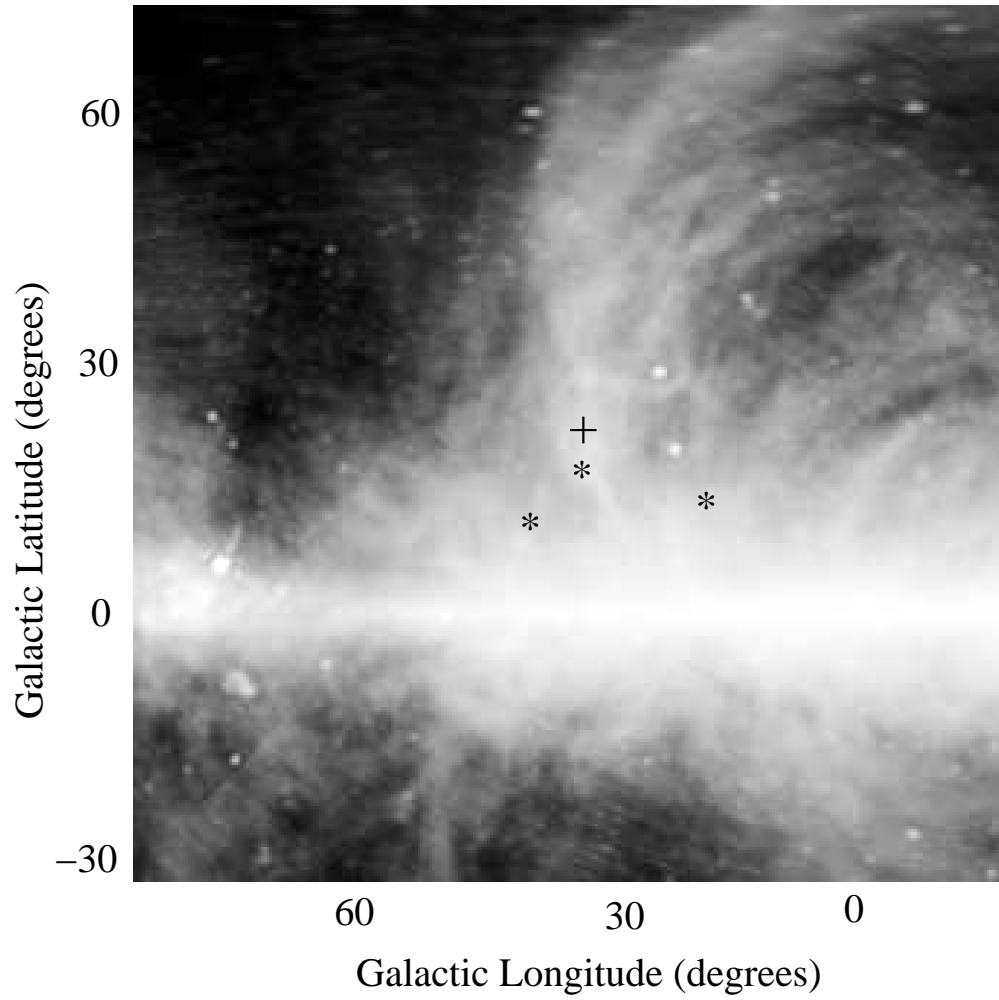


Fig. 9.— A  $105^\circ \times 105^\circ$  image of the Galaxy at 408 MHz, showing the NPS rising from the Galactic plane (Haslam et al. 1982). The position of PSR J1740+1000 is denoted with a cross. The positions of the three Extreme Scattering Event Sources associated with the NPS are denoted with asterisks.